On Simple Energy–Complexity Relations for Filament Tangles and Networks

Renzo L. Ricca

Department of Mathematics and Applications
U. Milano-Bicocca
Via Cozzi 53, 20125 Milano, Italy
renzo.ricca@unimib.it
http://www.matapp.unimib.it/~ricca

Structural complexity emerges from all systems that display morphological organization. Structural complexity for an intricate tangle of filaments is measured by the average crossing number of the tangle. Direct relationships between total length, energy, and structural complexity of a tangle are established. These results are based on elementary considerations that suggest a wide range of applications from magnetic energy estimates to neural and social networks and financial markets analysis.

1. Introduction

Structural organization is just one way to identify universal properties and whatever hidden mechanisms lie under this organization. Uncovering possible relations between generic properties of structural complexity and physical information is clearly of great importance [1, 2]. Progress in this direction gives us new ways to correlate localization and the occurrence of apparently distinct physical and mathematical properties that may reveal an unexpected new order of things, perhaps at a more fundamental level. Indeed, progress in understanding and detecting levels of complexity in physical or biological systems may help us to uncover new paradigmatic orders of complexity in the emerging mathematical structures.

Structural complexity [3] emerges from all systems that display morphological organization. Filamentary structures are one important example of coherent structures that emerge, interact, and evolve in many physical, biological (and social) systems, such as mass distribution in the universe, vortex filaments in turbulent flows, neural networks in our brain, and genetic material in a cell. In many cases, we expect that information on the degree of morphological order (or disorder) present in the system might tell us something important about fundamental physical or biological processes. It is well known, for instance, that the rate of energy dissipation in the bulk of a fluid depends crucially on how vorticity is distributed in that fluid; likewise, in brain research a high degree of isotropic intricacy in three-

Complex Systems, **20**
https://doi.org/10.25088/ComplexSystems.20.3.195

dimensional neural networks seems to guarantee high efficiency in the elaboration of signals.

For an intricate tangle of filaments, structural complexity is measured by the average crossing number of the tangle (see Section 2). Direct relationships between total length, energy, and structural complexity of a tangle are established in Section 3. These results are based on elementary expressions that suggest a wide range of validity and applicability. Immediate applications include energy estimates for magnetic fields, in particular solar coronal fields (Section 4). Future applications may include neural networks, social networks, and financial markets analysis (Section 5).

2. Extracting Information by Structural Complexity Methods

Structural complexity analysis aims at relating fundamental physical or biological aspects of a complex system with the mathematical description of the morphological complexity that the system exhibits. Information on structural complexity is based on a morphological and dynamical study of the constituents, utilizing applications of geometric, topological, and algebraic methods on one hand, and by dynamical systems analysis on the other [2, 4].

For a tangle of filaments given by a network of space curves, geometric measures of structural complexity are given, for example, by tropicity, coiling and alignment of the constituent filaments, and signed area information of the corresponding projected diagrams. Algebraic measures are given by average crossing number information of the apparent crossings present in the tangle. Topological measures are given by the linking numbers associated with the tangle components, as well as their minimal crossing numbers [5]. Dynamical system analysis provides information on topological entropy and eigenvalues of tensor fields that, in turn, can be profitably interpreted in terms of Minkowski functionals and shapefinders [6].

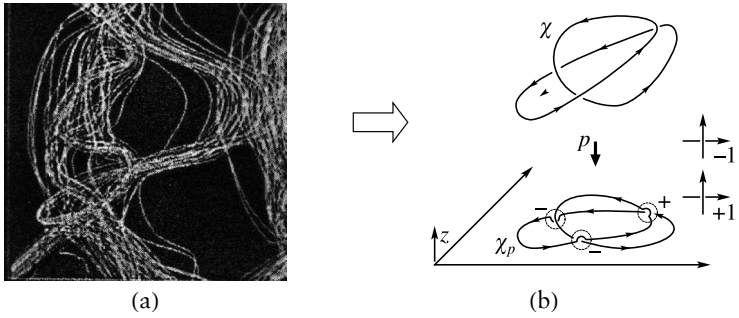

Figure 1. (a) Extracting information from experimental or numerical domains. (b) Structural complexity measures are obtained by diagram analysis on projected graphs from data produced by experimental or numerical work.

https://doi.org/10.25088/ComplexSystems.20.3.195

Given a tangle $\mathcal{T} = \bigcup_i \chi_i$ of n filaments χ_i, we consider the indented diagram $\mathcal{T}_p$ obtained by projecting $\mathcal{T}$ onto a plane of projection along a given direction p. For a single component χ (dropping the index), we consider the indented curve χ_p, resulting from the projection of χ (its geometric support) along p, keeping track of its topology by assigning $\epsilon_r = \pm 1$ to each underpass or overpass, at each apparent crossing site r, according to standard convention (see Figure 1). Evidently, this can be extended to any pair of curves by considering $r \in \chi_i \sqcap \chi_j$ for any pair $\{i, j\}$, and then to the whole tangle. Crossing counts on the indented diagrams prove useful for extracting geometric, algebraic, and topological information of the original tangle. In particular, we have the following definition.

Definition 1. The degree of structural complexity of a given tangle $\mathcal{T} = \bigcup_i \chi_i$ of n filaments χ_i $(i = 1, \ldots, n)$ is measured by the average crossing number $\overline{C}$ of the tangle, given by

$$\overline{C} \equiv \sum_{i,j} \int_{\chi_i} \int_{\chi_j} \frac{\left|(\mathbf{X}_i - \mathbf{X}_j) \cdot d\mathbf{X}_i \times d\mathbf{X}_j\right|}{\left|\mathbf{X}_i - \mathbf{X}_j\right|^3} = \sum_{r \in T} \left\langle \sum_{r \in \chi_i \sqcap \chi_j} |\epsilon_r| \right\rangle. \tag{1}$$

The definition of average crossing number was introduced by Freedman and He [7] and its interpretation in terms of average crossing count was proven by Ricca and Nipoti [8, 9]. The definition of structural complexity in terms of average crossing number was introduced by Ricca in 2005 [3].

As Moffatt and Ricca [10] demonstrated, the integral of equation (1) admits interpretation in terms of solid angle. To see this, consider the projection along p of a pair of curves χ_i, χ_j (the same argument applies to any pair of arcs of the same curve χ_i). Apparent intersections are counted by a number $r_+(p)$ and $r_-(p)$ of positive and negative crossings, respectively. The elements $d\mathbf{X}_i$, $d\mathbf{X}_j$ intersect in projection if and only if the p-direction is parallel to $\pm\left(\rho + \alpha d\mathbf{X}_i - \beta d\mathbf{X}_j\right)$ where $\rho = \mathbf{X}_i - \mathbf{X}_j$ (see Figure 2), $0 < \alpha < 1$, and $0 < \beta < 1$, that is, only if the p-direction lies within the elementary solid angle

$$\mathrm{d}\omega = 2\left(d\mathbf{X}_i \times d\mathbf{X}_j\right) \cdot \frac{\rho}{4\pi\rho^3}, \tag{2}$$

where $\rho = |\boldsymbol{\rho}|$ (the factor 2 allows for the $\pm$ possibilities). Thus, when we average over all directions of projections, taking into account the absolute value and then integrating over all pairs of elements $d\mathbf{X}_i$, $d\mathbf{X}_j$, we obtain

$$\overline{C}_{ij} = \frac{1}{4\pi} \int_{\chi_i} \int_{\chi_j} \frac{\left|\boldsymbol{\rho}\right| \cdot \left|d\mathbf{X}_i \times d\mathbf{X}_j\right|}{\rho^3} = \langle r_+(p) + r_-(p) \rangle, \tag{3}$$

https://doi.org/10.25088/ComplexSystems.20.3.195

that is,

$$\overline{C}_{ij} = \left\langle \sum_{r \in \chi_i \sqcap \chi_j} |\epsilon_r| \right\rangle, \tag{4}$$

where the angular brackets denote averaging over all directions p of projection. This gives an interpretation of equation (1) in terms of the average number of apparent (and unsigned) crossings.

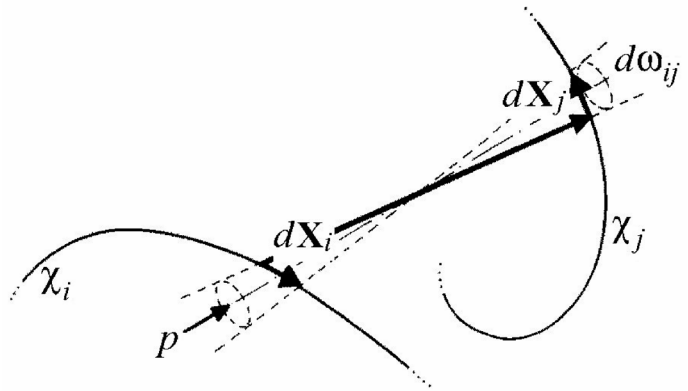

Figure 2. Solid angle interpretation of an apparent crossing. Two arcs of curve may be seen to cross each other when they are viewed along a direction of sight p. The apparent crossing is captured by the elementary solid angle contribution $d\omega_{ij}$, given by the relative position of the elementary vectors $d\mathbf{X}_i$ and $d\mathbf{X}_j$ in space.

This measure can be naturally extended to the whole tangle $\mathcal{T}$, that is,

$$\overline{C} = \sum_{\chi_i, \chi_j \in \mathcal{T}} \overline{C}_{ij}. \tag{5}$$

Equation (5) provides the most natural measure of structural complexity of $\mathcal{T}$, since it relates the degree of entanglement to an apparent localization of the number of crossings.

3. Energy–Complexity Relations for Filament Tangles and Networks

3.1 A Test Case: Superfluid Vortex Tangles

Work on superfluid vortex tangles has provided reliable test cases for investigating generic relationships between structural complexity and physical information. Complex tangles of vortex filaments have been

https://doi.org/10.25088/ComplexSystems.20.3.195

produced by direct numerical simulation methods (e.g., by superimposing an ABC flow on an initial vorticity distribution [11], or by spontaneous generation of a turbulent state [12]). Figure 3 shows a snapshot of a superfluid vortex tangle produced under an ABC-type flow action, as in [11].

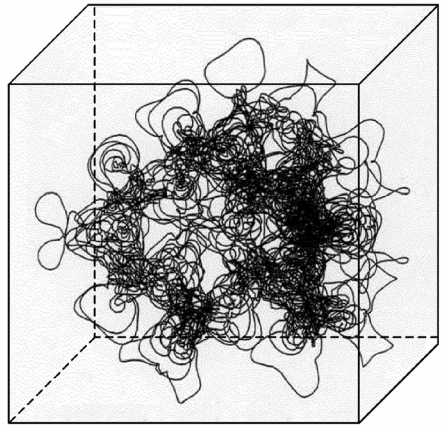

Figure 3. A superfluid vortex tangle produced by direct numerical simulation under an ABC-type flow action [11].

Results obtained by different methods and in different contexts have consistently indicated that structural complexity $\overline{C}$, total length $\overline{L}$, and total kinetic energy $\overline{E}$ of filaments relate according to

$$\overline{C} \sim \overline{L}^2 \quad \text{and} \quad \overline{C} \sim \overline{E}^2, \tag{6}$$

where $\overline{L} = L/L_0$ and $\overline{E} = E/E_0$ are nondimensional length and energy, respectively; L_0 and E_0 denote some reference values, for example, initial values. In what follows, we provide an elementary proof of the two relationships in equation (6). To this end, we consider the case of polygonal curves, since these are the real objects in numerical simulations.

3.2 Polygonal (Piecewise Linear) Space Curves

Consider the following experiment: take a number N of sticks of the same length and drop one stick at a time from some height onto a table top (see Figure 4(a)). Some sticks will pile up and some will inevitably fall away. We may ask: what is the maximum number of apparent crossings that can result from the piling process? The first three columns of Table 1 indicate the number of sticks/segments, the largest possible increase in the number of crossings Δc, and the maximum number of apparent crossings c obtained from each additional

https://doi.org/10.25088/ComplexSystems.20.3.195

stick dropped. As we see,

$$c = \frac{N}{2}(N-1) \Rightarrow c \sim N^2 \quad \text{as} \quad N \to \infty. \tag{7}$$

Now, instead of a single-plane projection, extend this experiment to all directions of projection and average out this measure with respect to the whole solid angle. The maximum number of crossings can now be replaced with its average value. Some of the sticks that do not contribute to the crossing count under a particular direction of projection might contribute when seen under a different direction of sight. Hence, by taking the average over all directions p, we have

$$\overline{C} = \langle c \rangle \sim N^2 \quad \text{as} \quad N \to \infty. \tag{8}$$

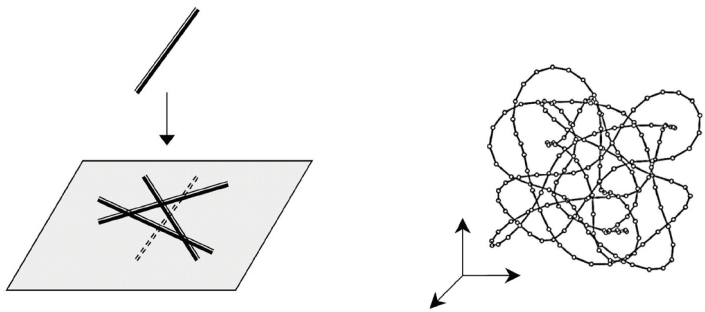

Figure 4. (a) Stick experiment: by dropping one stick at a time onto a table top, we can count the number of apparent crossings. (b) Polygonal curve in space.

Number of Sticks or Segments	Stick Experiment		Polygonal Curve
	max. Δc	max. c	max. c
1	0	0	0
2	1	1	0
3	2	3	1
4	3	6	3
5	4	10	6
6	5	15	10
...	...	...	...
$N+1$	N	$N(N-1)/2$	$N(N-1)/2$

Table 1. Crossing counts by stick experiment and by polygonal curve construction. The increase in the maximum number of apparent crossings c obtained by dropping sticks or adding segments follows the same law.

https://doi.org/10.25088/ComplexSystems.20.3.195

Now, consider the case of polygonal curves constructed by placing at random a segment in space and by adding consecutive, contiguous segments, as in Figure 4(b). We assume that all segments have the same length and each segment has its direction chosen at random in space or prescribed by some dynamical process. In doing this, we must ensure that the generating algorithm forbids complete overlapping of segments by prescribing a minimum angle between contiguous segments to avoid complete superimposition. Additional requirements, such as random spatial sampling, would enforce homogeneous isotropicity of the disordered tangle.

By directly inspecting the crossing count, the last column of Table 1 shows that for polygonal curves, the increase in the maximum number of crossings c follows the same rule as the stick experiment. Indeed, the first two segments just help to identify a plane of reference for the crossing count of all subsequent segments. Hence, by averaging crossings over all directions of sight, we again obtain the relationship $\overline{C} \sim N^2$ as $N \to \infty$. If all segments have the same length, and the energy per unit length is constant (or uniform due to an averaging process over the whole tangle), then for large N we have

$$\text{(i)}\ \overline{C} \sim \overline{L}^2, \qquad \text{(ii)}\ \overline{C} \sim \overline{E}^2. \tag{9}$$

4. Topological Complexity and Magnetic Energy

Foundational aspects in topological field theory call for more work on topological complexity, where topological properties are expected to play an important role at a fundamental energy level. Indeed, in ideal conditions (i.e., ideal magnetohydrodynamics) the magnetic energy M of (zero-framed) knotted flux tubes $\mathcal{K}$ of equal and constant magnetic flux Φ and total volume $V = V(\mathcal{K})$ is shown to be bounded from below by knot complexity. In particular, if the magnetic energy is given by

$$M = \int_{V(\mathcal{K})} \|\mathbf{B}\|^2 \, d^3\,\mathbf{x}, \tag{10}$$

where $\mathbf{B}$ is the magnetic field confined to the tube, then, by using previous results by Arnold (1974), Moffatt (1990), and Freedman and He (1991), one can prove [13] that

$$M_{\min} = \left(\frac{16}{\pi}\right)^{1/3} \frac{\Phi^2}{V^{1/3}}\, c_{\min}, \tag{11}$$

that is,

$$M_{\min} \propto c_{\min}, \tag{12}$$

https://doi.org/10.25088/ComplexSystems.20.3.195

where $c_{\min}$ is the minimum number of crossings of the knot (or link) type $\mathcal{K}$, $c_{\min}$ being a topological invariant of $\mathcal{K}$. Another important quantity of topological character (related to the linking number) is the magnetic helicity H [10], given by

$$H = \int_{V(\mathcal{K})} \mathbf{A} \cdot \mathbf{B}\, d^3\,\mathbf{x}, \tag{13}$$

where $\mathbf{B} = \nabla \cdot \mathbf{A}$ (with $\nabla \cdot \mathbf{A} = 0$). Then, we have

$$M \geq \left(\frac{16}{\pi\, V}\right)^{1/3} |H|. \tag{14}$$

However, in the presence of dissipation, magnetic fields reconnect and the change in topology is reflected in the change of topological complexity according to

$$H(t) \leq 2\,\Phi^2\,\overline{C}(t), \tag{15}$$

where inequality provides an upper bound on the magnetic helicity by the average crossing number of the magnetic system.

5. Outlook: From Neural and Social Networks to Financial Markets Analysis

The relationships in equation (9) are based on expressions of some general validity and applicability that suggest possible applications in different contexts. The complexity of three-dimensional networks of filamentary structures in biology provides an example as evidenced by the intricacy of embryonic fibroblasts or retina astrocytes *in vivo*. Direct imaging analysis based on digital acquisition of the morphological complexity in such networks allows extracting the average crossing number information rather efficiently. This information allows for quantifying properties such as total length and length density of the filament network, as well as estimating corresponding energy aspects (electric current or signal information) present in the network or in particular subregions of it. The density and space localization of the apparent crossings also allows for evaluating the efficiency of agents (e.g., nerve growth factors for neural networks) and signal elaboration on local or global scales, possibly identifying critical conditions.

Similarly, analysis of information in social networks, financial markets, and insurance products can be facilitated by extracting average crossing number information from the entanglement of links or actions in the appropriate phase portrait. For example, in the case of insurance analysis against rare catastrophic events, the crossing number information can be profitably related to critical properties associated with the high localization of apparent crossings at a given moment in

https://doi.org/10.25088/ComplexSystems.20.3.195

time, a measure that, in turn, can be put in relation to capital or risk investments.

Acknowledgments

I wish to express my gratitude to the Mathematical Research Center (CRM) "Ennio de Giorgi" of the Scuola Normale Superiore in Pisa, for their kind hospitality during the preparation of this work.

References

[1] C. Song, S. Havlin, and H. A. Makse, "Self-Similarity of Complex Networks," *Nature*, **433**, 2005 pp. 392–395. doi:10.1038/nature03248.

[2] R. L. Ricca, "Detecting Structural Complexity: From Visiometrics to Genomics and Brain Research," in *Mathknow* (M. Emmer and A. Quarteroni, eds.), Heidelberg: Springer-Verlag, 2009 pp. 167–181.

[3] R. L. Ricca, "Structural Complexity," in *Encyclopedia of Nonlinear Science* (A. Scott, ed.), New York and London: Routledge, 2005 pp. 885–887.

[4] R. H. Abraham and C. D. Shaw, *Dynamics: The Geometry of Behavior*, Addison-Wesley, 1992.

[5] R. L. Ricca, "Structural Complexity and Dynamical Systems," in *Lectures on Topological Fluid Mechanics (CIME Summer School '01)*, Cetraro, Italy (R. L. Ricca, ed.), Berlin: Springer-Verlag, 2009 pp. 179–199.

[6] R. L. Ricca, "New Developments in Topological Fluid Mechanics," *Il Nuovo Cimento C*, **32**(1), 2009 pp. 185–192. doi:10.1393/ncc/i2009-10355-2.

[7] M. H. Freedman and Z.-X. He, "Divergence-Free Fields: Energy and Asymptotic Crossing Number," *Annals of Mathematics*, **134**(1), 1991 pp. 189–229. http://www.jstor.org/pss/2944336.

[8] R. L. Ricca and B. Nipoti, "Derivation and Interpretation of the Gauss Linking Number," in *Introductory Lectures on Knot Theory* (L. H. Kauffman, S. Lambropoulou, S. Jablan, and J. H. Przytycki, eds.), Singapore: World Scientific, 2011 pp. 482–501.

[9] R. L. Ricca and B. Nipoti, "Gauss' Linking Number Revisited," *Journal of Knot Theory and Its Ramifications*, **20**(10), 2011 pp. 1325–1343. doi:10.1142/S0218216511009261.

[10] H. K. Moffatt and R. L. Ricca, "Helicity and the Călugăreanu Invariant," *Proceedings of the Royal Society of London A*, **439**(1906), 1992 pp. 411–429. doi:10.1098/rspa.1992.0159.

[11] C. F. Barenghi, R. L. Ricca, and D. C. Samuels, "How Tangled Is a Tangle?" *Physica D*, **157**(3), 2001 pp. 197–206. doi:10.1016/S0167-2789(01)00304-9.

https://doi.org/10.25088/ComplexSystems.20.3.195

[12] D. R. Poole, H. Scoffield, C. F. Barenghi, and D. C. Samuels, "Geometry and Topology of Superfluid Turbulence," *Journal of Low Temperature Physics*, **132**(1), 2003 pp. 97–117. doi:10.1023/A:1023797226059.

[13] R. L. Ricca, "Topology Bounds Energy of Knots and Links," *Proceedings of the Royal Society of London A*, **464**(2090) 2008 pp. 293–300. doi:10.1098/rspa.2007.0174.

https://doi.org/10.25088/ComplexSystems.20.3.195